


 Cite this: *RSC Adv.*, 2026, 16, 4299

## Harnessing Frémy's salt for tyrosine-directed bioconjugations

 Zachary V. Samuels,<sup>1</sup> Ava Stoddard,<sup>2,3</sup> Wei-Siang Mark Kao,<sup>4,5</sup> Mike A. Cornejo,<sup>6,7</sup> Emilia Strugala,<sup>8</sup> Shane A. McGlone,<sup>8</sup> Lauren Furer,<sup>8</sup> Cindy Rodriguez<sup>9,10</sup> and Brian M. Zeglis<sup>11</sup>

 Received 29th August 2025  
 Accepted 28th December 2025

DOI: 10.1039/d5ra06489a

[rsc.li/rsc-advances](https://rsc.li/rsc-advances)

The current bioconjugation toolbox overwhelmingly comprises strategies that modify lysine and cysteine residues within proteins and peptides. Herein, we have leveraged Frémy's salt (potassium nitrosodisulfonate) to create an approach to bioconjugation predicated on the oxidation of tyrosine residues and the subsequent strain-promoted oxidation-controlled quinone ligation between the resultant 1,2-quinones and *trans*-cyclooctene-bearing cargoes.

Over the last three decades, protein- and peptide-based bioconjugates have become indispensable tools in both the laboratory and the clinic. Their utility, especially within oncology, is predicated on combining the exquisite affinity and selectivity of biomolecules for molecular targets of disease and the unique properties of small molecules. For example, antibody–drug conjugates (ADCs)—as their name suggests—are unions of immunoglobulins (*e.g.* trastuzumab) and toxins (*e.g.* deruxtecan) that are widely employed for the targeted therapy of cancer.<sup>1,2</sup> In addition, many diagnostic and therapeutic radiopharmaceuticals are combinations of radiometal chelators and receptor-specific peptides; to wit, the recently FDA-approved Lutathera™ features DOTA attached to a somatostatin receptor-targeting peptide.<sup>3</sup> Beyond these high-profile examples, a myriad of bioconjugates (especially antibodies attached to fluorophores) are used as molecular tools in the laboratory.

The process by which these molecular tools are created is called 'bioconjugation'. Traditionally, the attachment of cargoes to biomolecules has been achieved *via* the stochastic modification of lysine (K) residues with amine-reactive synthons like *N*-hydroxysuccinimidyl (NHS) esters or isothiocyanates. However, these strategies sacrifice control over the molecular location of the reaction if biomolecules have more than one lysine. As a result, stochastic bioconjugation can

yield heterogeneous and poorly-defined conjugates with—if the modification occurs within a critical domain—impaired *in vitro* and *in vivo* performance.<sup>4</sup>

To circumvent this problem, investigators have increasingly turned to site-selective and site-specific approaches to bioconjugation.<sup>5</sup> A wide variety of these strategies have been developed, including variants based on click chemistry, chemoenzymatic transformations, and the manipulation of glycans chains.<sup>6</sup> However, the most popular (and most facile) methods are based on the attachment of cargoes to the sulfhydryl groups of cysteine residues—often the reduced interchain disulfides of immunoglobulins—using thiol-reactive moieties like malimides or phenylloxadiazolyl methylsulfones.<sup>7</sup>

The primacy of lysine and cysteine residues in bioconjugation can pose a problem if the biomolecule does not contain either residue or, alternatively, if the residues in question lie in particularly important structural or functional domains. Consequently, there has been significant interest in the development of bioconjugation strategies that selectively target other amino acids.<sup>8</sup> Along these lines, tyrosine (Y) is a particularly promising target due to its low abundance on the surface of proteins and the reactivity conferred by its phenol group.<sup>9–12</sup>

Several tyrosine-directed approaches to bioconjugation have been created, each with its own set of advantages and disadvantages.<sup>13–15</sup> In 2004, for example, Joshi, *et al.* leveraged a three-component Mannich-type reaction between tyrosine's phenol group, an aldehyde, and a cargo-bearing aniline as a versatile and cost-effective route to tyrosine-based protein modification.<sup>16</sup> However, the inadvertent modification of tryptophan residues during this reaction can reduce the specificity of this approach to bioconjugation.<sup>17</sup> In 2014, Ban *et al.* developed a strategy predicated upon the reaction of oxidation-activated cyclic diazocarbonylamides like 4-phenyl-3*H*-1,2,4-triazoline-3,5(4*H*)-diones (PTADs) with tyrosine.<sup>18</sup> Like the

<sup>1</sup>Department of Chemistry, Hunter College, City University of New York, New York, NY, 10065, USA. E-mail: bz102@hunter.cuny.edu

<sup>2</sup>PhD Program in Chemistry of the Graduate Center of the City University of New York, New York, NY, 10016, USA

<sup>3</sup>Department of Radiology, Memorial Sloan Kettering Cancer Center, New York, NY, 10065, USA

<sup>4</sup>PhD Program in Biology of the Graduate Center of the City University of New York, New York, NY, 10016, USA

<sup>5</sup>PhD Program in Biochemistry of the Graduate Center of the City University of New York, New York, NY, 10016, USA

<sup>6</sup>Department of Radiology, Weill Cornell Medical College, New York, NY, 10065, USA


Mannich-type strategy developed a decade earlier, this method has been employed to synthesize a variety of bioconjugates; however, the PTADs can decompose into isocyanates, resulting in side-reactions with primary amines. Just this year, the Francis group at the University of California Berkeley has developed a three-step chemoenzymatic approach based on the tyrosinase-mediated oxidation of tyrosines to 1,2-quinones, the modification of these quinones with dithiothreitol to introduce thiol moieties, and the subsequent modification of these sulfhydryl groups with maleimide-bearing probes.<sup>19</sup> This innovative approach creatively facilitates the modification of tyrosine residues with thiol-reactive probes, but its use of an enzyme (*i.e.* tyrosinase) could create problems in the context of clinical production.

We have previously developed an approach to the site-specific modification of antibodies based on (i) the deglycosylation of the immunoglobulin with PNGaseF; (ii) the oxidation of a quartet of exposed tyrosine residues (*i.e.* Y296 and Y300 on each heavy chain) with mushroom tyrosinase; and (iii) the strain-promoted oxidation-controlled quinone (SPOCQ) ligation between the resultant quinones and TCO-bearing cargoes.<sup>20</sup> This strategy proved highly effective, yielding homogeneous, well-defined, and stable <sup>89</sup>Zr-DFO-labeled radio-immunoconjugates with excellent *in vivo* performance in a murine model of colorectal carcinoma. However, this method's use of two different enzymes is problematic on two levels. First, the enzymatic incubations are lengthy (6 and 18 h, respectively). And second, the incorporation of enzymes into the GMP clinical production of probes can be very challenging.

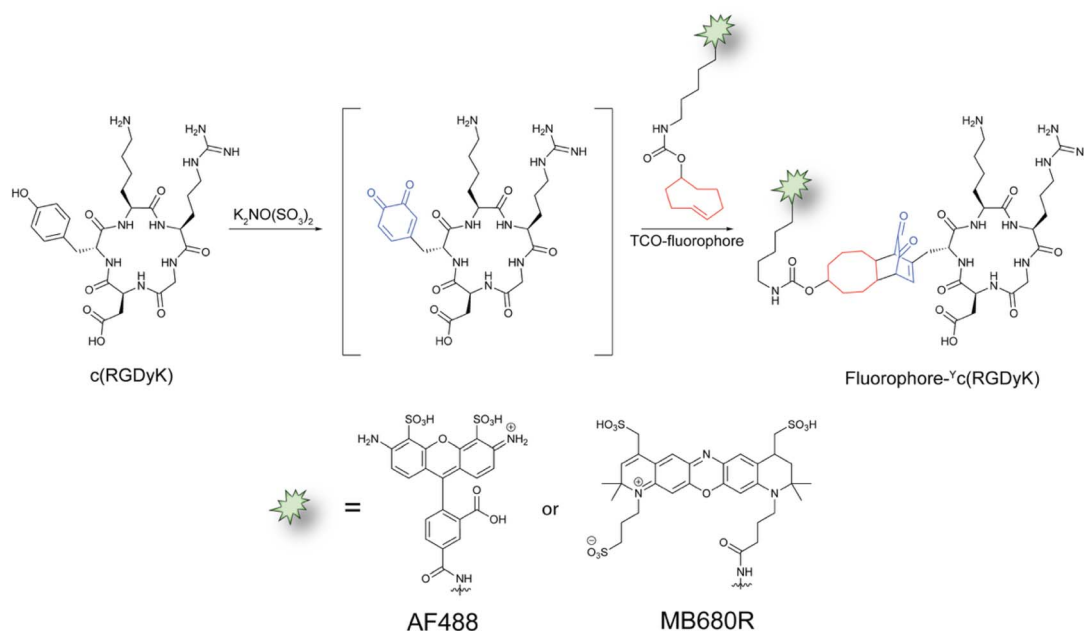
In light of these challenges, we have worked to develop an approach to tyrosine-directed bioconjugation that eschews the enzymatic oxidation of the amino acids (Scheme 1). To this end,

we have turned to Frémy's salt (potassium nitrosodisulfonate, discovered by the eponymous Frenchman in 1845), a long-lived radical that has been used in a variety of applications and was shown to oxidize aromatic hydroxyls into quinones in 1971 by Zimmer, *et al.*<sup>21–24</sup> Furthermore, it is inexpensive, commercially available, water soluble, and easier to remove from reaction solutions than its enzymatic counterparts. A similar approach has been explored in the past, but the investigation in question used a different dienophile (*i.e.* bicyclononyne), did not include any comparative studies to traditional lysine-mediated bioconjugation, and did not include any *in vivo* evaluation experiments.<sup>18</sup>

To validate this approach to bioconjugation, we chose a model system based on the  $\alpha_v\beta_3$  integrin-binding c(RGDyK) peptide. Imaging agents based on this peptide are very well characterized both *in vitro* and *in vivo*, and—*even more importantly*—the peptide contains both tyrosine and lysine residues outside of its RGD binding motif, allowing us to directly compare this nascent method to bioconjugation to traditional, K-mediated techniques.<sup>25</sup>

The first step in the development of this system was validating the ability of Frémy's salt to oxidize the peptide's tyrosine to a 1,2-quinone. To this end, Frémy's salt (1.7 mg; 6.3  $\mu$ mol) was added to a solution of the peptide in PBS buffer (6 mM), and the absorbance of the solution at 280 and 380 nm was monitored over the course of 60 min (Fig. 1). Critically, time-dependent changes in absorbance at 280 and 380 nm were observed, a well-established hallmark of the conversion of a phenol to a 1,2-quinone.<sup>26,27</sup>

The SPOCQ ligation is predicated on the reaction of 1,2-quinones with dienophiles such as *trans*-cyclooctene (TCO).<sup>28–30</sup> For this investigation, we turned to TCO-bearing variants of two



**Scheme 1** The synthesis of fluorophore-modified peptides *via* the oxidation of a tyrosine residue with Frémy's salt and the subsequent SPOCQ ligation between the resultant 1,2-quinone and a TCO-bearing cargo.



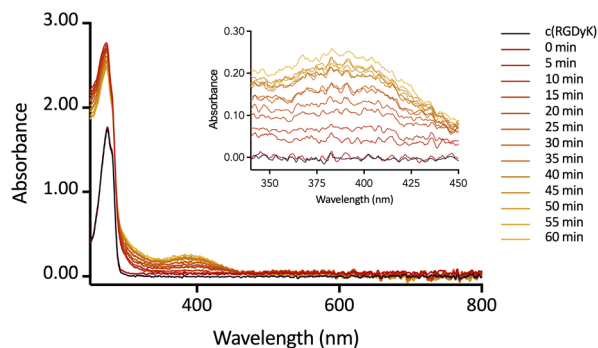


Fig. 1 UV-vis absorbance spectra of c(RGDyK) collected for 60 minutes after the addition of Frémy's salt. Inset: the absorbance at 380 nm over the same period.

rhodamine-based fluorophores: the green-light emitting AlexaFluor™ 488 (AF488) and the near-infrared emitting MB680R. With respect to the former, a TCO-bearing analogue of AF488 was purchased from VectorLabs (Newark, California). With respect to the latter, MB680R-NHS (5 mg; 6  $\mu$ mol) was dissolved in DMF (600  $\mu$ L) and then combined with TCO-NH<sub>2</sub> HCl (3.1 mg; 12  $\mu$ mol) and DIPEA (3 mg; 24  $\mu$ mol). The resultant solution was then stirred at RT for 60 min, during which the progress of the reaction was monitored *via* RP-HPLC. Upon completion, the reaction was purified *via* preparative RP-HPLC, yielding the completed fluorophore—TCO-MB680R—in >99% purity and a yield of 64–75% (Fig. S1).

With the TCO-bearing fluorophores in hand, we proceeded to the bioconjugation reaction itself. Here, each TCO-fluorophore (2 mg; 2.1–2.6  $\mu$ mol) was combined with c(RGDyK) (1.5 eq.) and Frémy's salt (4 eq.) in 700  $\mu$ L of a 50% acetonitrile/tris buffer solution (pH 8) and stirred on ice for 1 h. The final conjugates—AF488-<sup>Y</sup>c(RGDyK) and MB680R-<sup>Y</sup>c(RGDyK)—were purified *via* preparative RP-HPLC and isolated in 60–70% yield, and the identity of AF488-<sup>Y</sup>c(RGDyK) ( $m/z$  [M + 2H]<sup>2+</sup> = 703.0) and MB680R-<sup>Y</sup>c(RGDyK) ( $m/z$  [M + 2H]<sup>2+</sup> = 792.5) was then confirmed *via* ESI-MS (Fig. S2 and S3). High-resolution mass spectrometry was performed for each compound: AF488-<sup>Y</sup>c(RGDyK) (expected = 1404.487; actual = 1404.494) and MB680R-<sup>Y</sup>c(RGDyK) (expected = 1583.622; actual = 1583.625) (Fig. S4 and S5).

In parallel, we also synthesized AF488- and MB680R-bearing variants of c(RGDyK) *via* traditional lysine-directed bioconjugation to facilitate comparisons between the two methods. In this case, NHS-bearing variants of each fluorophore (2.5 mg; 3.0–4.0  $\mu$ mol) were combined with c(RGDyK) (1.5 eq.) and DIPEA (4 eq.) in 300  $\mu$ L of DMF and stirred at RT for 1 h. In line with the preparation of the first pair, the final conjugates—AF488-<sup>K</sup>c(RGDyK) and MB680R-<sup>K</sup>c(RGDyK)—were purified *via* preparative RP-HPLC and isolated in 60–90% yield, and their identity was confirmed *via* ESI-MS (Fig. S6 and S7). High-resolution mass spectrometry was also performed for each compound: AF488-<sup>K</sup>c(RGDyK) (expected = 1136.309; actual = 1136.312) and MB680R-<sup>K</sup>c(RGDyK) (expected = 1343.474; actual = 1343.481) (Fig. S8 and S9). Each K- or Y-linked bioconjugate

was incubated in phosphate-buffered saline (pH 7.4) at 37 °C for 7 days, and the integrity of the probes was assessed daily *via* analytical HPLC. All four conjugates remained >96% pure over the course of the experiment (Fig. S10).

To better understand the relative fluorescence of our probes, 5  $\mu$ M solutions of each conjugate were added to a clear-bottom 96-well plate (100  $\mu$ L per well;  $n$  = 7) and analyzed with a microplate fluorescence detector. The relative fluorescence of AF488-<sup>Y</sup>c(RGDyK) ( $1.1 \times 10^9 \pm 1.6 \times 10^7$  RFU) was about 5% greater than that of AF488-<sup>K</sup>c(RGDyK) ( $9.9 \times 10^8 \pm 1.6 \times 10^7$  RFU) using excitation and emission wavelengths of 494 and 517 nm, respectively. Moving on to the other pair, the fluorescence of MB680R-<sup>Y</sup>c(RGDyK) ( $6.9 \times 10^7 \pm 4.3 \times 10^6$  RFU) was nearly 25% more intense than that of MB680R-<sup>K</sup>c(RGDyK) ( $5.5 \times 10^7 \pm 3.1 \times 10^6$  RFU) using excitation and emission wavelengths of 685 and 709 nm, respectively. The origin of this phenomenon almost certainly lies in the established ability of tyrosine residues—which are present in the K-linked variants but not the Y-linked probes—to quench the fluorescence of rhodamine-based fluorophores.<sup>31–33</sup>

The literature clearly illustrates that the RGD motif of this family of peptides is responsible for their affinity for  $\alpha_v\beta_3$  integrin and that neither modifying nor replacing the Y- or K-residues of c(RGDyK) significantly interferes with binding.<sup>34,35</sup> However, we nonetheless performed *in vitro* experiments with  $\alpha_v\beta_3$  integrin-expressing cells in order to ensure that the modification of the tyrosine residue did not substantially impede the peptide's ability to bind its target. For this assay, we employed the AF488-labeled peptides, as the visible light emission from this fluorophore is compatible with our confocal laser scanning microscope (CLSM). U-87 MG human glioblastoma cells were seeded on microscope slides, stained with both DAPI (35  $\mu$ M) and either AF488-<sup>K</sup>c(RGDyK) or AF488-<sup>Y</sup>c(RGDyK) (10  $\mu$ M), fixed with formalin, mounted with a fluorescence-preserving mounting medium, and imaged with a CLSM using identical acquisition settings (see SI Methods for details). Importantly, both conjugates clearly bind to the  $\alpha_v\beta_3$  integrin-expressing cells, with the signal from AF488-<sup>Y</sup>c(RGDyK) noticeably more intense than that from AF488-<sup>K</sup>c(RGDyK) at similar cellular densities (Fig. 2).

The final step in the investigation was the comparative evaluation of the *in vivo* behaviour of the K- and Y-linked imaging agents. For these experiments, we turned to the MB680R-bearing probes, as the NIR emission from this fluorophore better penetrates tissue and lies farther from the wavelength of any natural (or feed-related) autofluorescence. Athymic mice bearing subcutaneous U-87 MG xenografts were injected with either MB680R-<sup>Y</sup>c(RGDyK) or MB680R-<sup>K</sup>c(RGDyK) [18–21  $\mu$ g (13 nmol) in 100  $\mu$ L of sterile PBS] *via* the lateral tail vein. *In vivo* images were then acquired 1, 4, and 24 h after the administration of the probes using a PerkinElmer IVIS Spectrum (Fig. 3A and S11). Immediately after the final timepoint, the animals were euthanized, the xenografts and selected organs were collected and arrayed, and an additional *ex vivo* NIRF image was acquired (Fig. 3B and S12). By 24 h p.i., both MB680R-<sup>Y</sup>c(RGDyK) or MB680R-<sup>K</sup>c(RGDyK) localize in the tumour and clearly delineate it from surrounding healthy



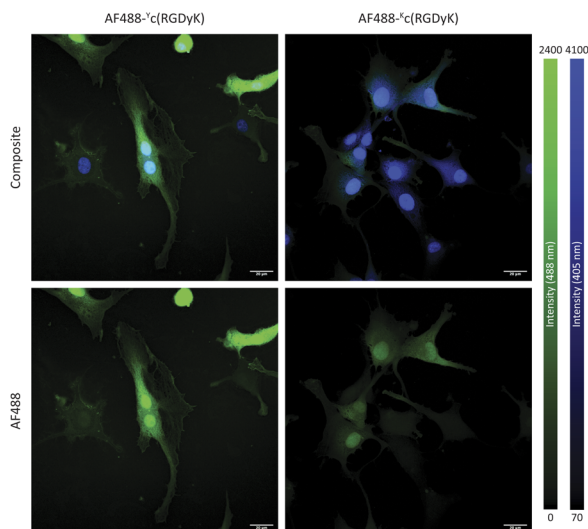


Fig. 2 CLSM of U-87 MG cells stained with AF488- $\gamma$ c(RGDyK) or AF488- $\kappa$ c(RGDyK) (green) and DAPI (blue).

tissue. Interestingly, there are two intriguing differences between the performance of the probes: in both the 24 h p.i. *in vivo* and *ex vivo* images, MB680R- $\gamma$ c(RGDyK) produces higher signal in both the tumour and the kidneys (Fig. 3C). These data suggest that while this tyrosine-based approach to bioconjugation does not impede the ability of the imaging agent to delineate target tissue, it can alter the pharmacokinetic profile of the probe compared to an analogue created using lysine-mediated bioconjugation. The differences in the *in vivo* behaviour of MB680R- $\gamma$ c(RGDyK) may be related to the elimination of the tyrosine's hydrogen-bonding capability, the presence of the bicyclic ring system, the presence of a free amine, or—most likely of all—a combination of these factors.

Before we conclude, we would be remiss if we did not address what appears to be a significant limitation of this strategy: the strength of the oxidant. During the investigation, we found that Frémy's salt is incompatible with several common near-infrared fluorophores. Indeed, both IR800CW and Cy5.5 quickly decomposed—as evidenced by a rapid change in colour—upon exposure to the salt (Fig. S13). In light of this phenomenon, we decided to explore the reactivity of Frémy's salt with several amino acids that are prone to oxidation, specifically phenylalanine, tryptophan, cysteine, and methionine. HPLC chromatograms of the former pair before and after incubation with Frémy's salt reveal that both are largely inert to the oxidant (Fig. S14 and S15). Cysteine and methionine lack chromophores, so AF488 conjugates of each—AF488-Cys and AF488-Met—were prepared to facilitate visualization *via* chromatography (Fig. S16 and S17). Subsequent HPLC analysis before and after treatment with Frémy's salt suggests that both amino acids are not readily oxidized by potassium nitrosodisulfonate but that some decomposition can be observed (Fig. S18 and S19). While these experiments did not uncover significant reactivity between these residues and Frémy's salt, the oxidant may still be too strong to use with more complex

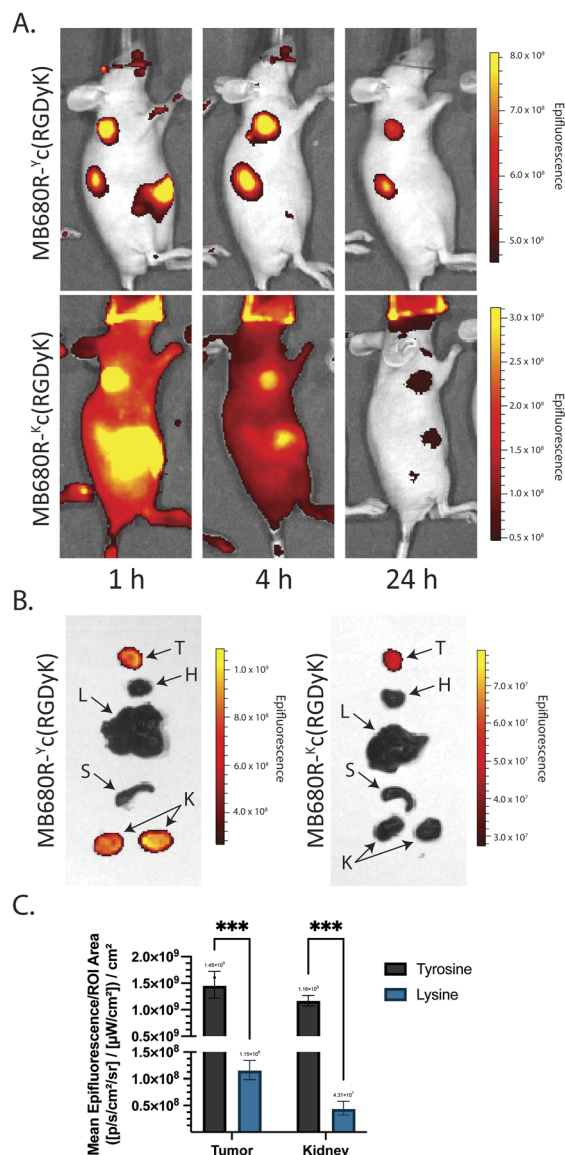


Fig. 3 (A) *In vivo* NIRF images acquired 1, 4, and 24 h after the administration of MB680R- $\gamma$ c(RGDyK) and MB680R- $\kappa$ c(RGDyK) to athymic nude mice bearing subcutaneous U-87 MG xenografts (right shoulder); (B) *ex vivo* NIRF images of selected organs acquired immediately after the final imaging time point (T = tumour; H = heart; L = liver; S = spleen; K = kidneys); (C) quantitative comparison of the tumour and kidney signal of the two imaging agents.

biomolecules like immunoglobulins. To wit, size-exclusion HPLC of a full-length IgG<sub>1</sub> (*i.e.* 5B1) treated with the salt revealed that higher concentrations of oxidant prompted the formation of a peak indicative of the aggregation of the biomolecule (Fig. S20). Clearly, while this method of tyrosine-targeted bioconjugation is effective, both the cargo and the vector with which it is used must be chosen carefully.

In conclusion, we have effectively demonstrated that Frémy's salt can be harnessed as part of a tyrosine-specific bioconjugation strategy predicated on the SPOCQ ligation. We have successfully used this approach to synthesize two highly stable  $\alpha_v\beta_3$  integrin-targeting fluorescence imaging agents:



AF488-<sup>Y</sup>c(RGDyK) and MB680R-<sup>Y</sup>c(RGDyK). Furthermore, we have demonstrated that these probes exhibit comparable (if not superior) *in vitro* and *in vivo* performance compared to analogous agents synthesized *via* traditional lysine-directed methods. Critically, however, we have also observed that Frémy's salt is such a strong oxidant that it can destroy certain fluorophores and damage certain biomolecules, suggesting that this method—while useful—may have limited scope as presently constituted. Efforts are underway to identify more mild chemical oxidants capable of converting tyrosines to 1,2-quinones, thereby enabling a gentler variation of this strategy.

## Ethical statement

All animal work was performed under the guidance and approval of the Institutional Animal Care and Use Committee (IACUC) of Weil Cornell Medical College (protocol number 2015-0004).

## Conflicts of interest

There are no conflicts to declare.

## Data availability

Data for this article—including chemical synthesis data, chemical characterization data, and *in vivo* images—have been included in the supplementary information (SI). Supplementary information (SI) is available. See DOI: <https://doi.org/10.1039/d5ra06489a>.

## Notes and references

- 1 S. Verma, D. Miles, L. Gianni, I. E. Krop, M. Welslau, J. Baselga, M. Pegram, D.-Y. Oh, V. Diéras, E. Guardino, L. Fang, M. W. Lu, S. Olsen and K. Blackwell, *N. Engl. J. Med.*, 2012, **367**, 1783–1791.
- 2 T. Powles, J. E. Rosenberg, G. P. Sonpavde, Y. Loriot, I. Durán, J.-L. Lee, N. Matsubara, C. Vulsteke, D. Castellano, C. Wu, M. Campbell, M. Matsangou and D. P. Petrylak, *N. Engl. J. Med.*, 2021, **384**, 1125–1135.
- 3 J. Strosberg, G. El-Haddad, E. Wolin, A. Hendifar, J. Yao, B. Chasen, E. Mittra, P. L. Kunz, M. H. Kulke, H. Jacene, D. Bushnell, T. M. O'Dorisio, R. P. Baum, H. R. Kulkarni, M. Caplin, R. Lebtahi, T. Hobday, E. Delpassand, E. V. Cutsem, A. Benson, R. Srirajaskanthan, M. Pavel, J. Mora, J. Berlin, E. Grande, N. Reed, E. Seregni, K. Öberg, M. L. Sierra, P. Santoro, T. Thevenet, J. L. Erion, P. Ruzniewski, D. Kwekkeboom and E. Krenning, *N. Engl. J. Med.*, 2017, **376**, 125–135.
- 4 B.-Q. Shen, K. Xu, L. Liu, H. Raab, S. Bhakta, M. Kenrick, K. L. Parsons-Reponte, J. Tien, S.-F. Yu, E. Mai, D. Li, J. Tibbitts, J. Baudys, O. M. Saad, S. J. Scales, P. J. McDonald, P. E. Hass, C. Eigenbrot, T. Nguyen, W. A. Solis, R. N. Fuji, K. M. Flagella, D. Patel, S. D. Spencer, L. A. Khawli, A. Ebens, W. L. Wong, R. Vandlen, S. Kaur, M. X. Sliwowski, R. H. Scheller, P. Polakis and J. R. Junutula, *Nat. Biotechnol.*, 2012, **30**, 184–189.
- 5 J. Sebastiano, Z. V. Samuels, W.-S. Kao and B. M. Zeglis, *Curr. Opin. Chem. Biol.*, 2024, **81**, 102471.
- 6 D. Bauer, M. A. Cornejo, T. T. Hoang, J. S. Lewis and B. M. Zeglis, *Bioconjug. Chem.*, 2023, **34**, 1925–1950.
- 7 P. Adumeau, M. Davydova and B. M. Zeglis, *Bioconjugate Chem.*, 2018, **29**, 1364–1372.
- 8 J. N. deGruyter, L. R. Malins and P. S. Baran, *Biochemistry*, 2017, **56**, 3863–3873.
- 9 D. Alvarez Dorta, D. Deniaud, M. Mével and S. G. Guoin, *Chem.–Eur. J.*, 2020, **26**, 14257–14269.
- 10 B. M. da S. Santos, L. C. R. M. da Frota, T. G. Silva and F. G. Finelli, *Chem. Rec.*, 2025, e202500215.
- 11 A. Chowdhury, S. Chatterjee, A. Pongen, D. Sarania, N. M. Tripathi and A. Bandyopadhyay, *Protein Pept. Lett.*, 2021, **28**, 788–808.
- 12 P. A. Szijj, K. A. Kostadinova, R. J. Spears and V. Chudasama, *Org. Biomol. Chem.*, 2020, **18**, 9018–9028.
- 13 J. J. Bruins, D. Blanco-Ania, V. van der Doef, F. L. van Delft and B. Albada, *Chem. Commun.*, 2018, **54**, 7338–7341.
- 14 S. Sato, S. Miyano, K. Nakane, Z. Liu, M. Kumashiro, T. Saio, Y. Tanaka, A. Shigenaga, C. Fujimura, E. Koyanagi, H. Nishi, S. Tomoshige and M. Ishikawa, *Tetrahedron Chem.*, 2024, **12**, 100111.
- 15 B. Albada, J. F. Keijzer, H. Zuilhof and F. van Delft, *Chem. Rev.*, 2021, **121**, 7032–7058.
- 16 N. S. Joshi, L. R. Whitaker and M. B. Francis, *J. Am. Chem. Soc.*, 2004, **126**, 15942–15943.
- 17 J. M. McFarland, N. S. Joshi and M. B. Francis, *J. Am. Chem. Soc.*, 2008, **130**, 7639–7644.
- 18 H. Ban, M. Nagano, J. Gavriljuk, W. Hakamata, T. Inokuma and C. F. I. Barbas, *Bioconjug. Chem.*, 2013, **24**, 520–532.
- 19 P. Huang, W. Cao, J. L. Fetzer, N. S. Dolan and M. B. Francis, *J. Am. Chem. Soc.*, 2025, **147**, 23834–23843.
- 20 C. Rodriguez, S. Delaney, J. Sebastiano, S. M. Sarrett, M. A. Cornejo, S. Thau, M. M. Hosny and B. M. Zeglis, *RSC Adv.*, 2023, **13**, 17705–17709.
- 21 W. Moser and R. A. Howie, *J. Chem. Soc. A*, 1968, 3039–3043.
- 22 H. Zimmer, D. C. Lankin and S. W. Horgan, *Chem. Rev.*, 1971, **71**, 229–246.
- 23 M. Wilchek and T. Miron, *Bioconjug. Chem.*, 2015, **26**, 502–510.
- 24 A. George, G. Krishna Priya, M. Ilamaran, N. R. Kamini, S. Ganesh, S. Easwaramoorthi and N. Ayyadurai, *ChemistrySelect*, 2017, **2**, 7117–7122.
- 25 S. Liu, *Bioconjug. Chem.*, 2009, **20**, 2199–2213.
- 26 G. Faccio, M. M. Kämpf, C. Piatti, L. Thöny-Meyer and M. Richter, *Sci. Rep.*, 2014, **4**, 5370.
- 27 K. Piechowska, M. Świtalska, J. Cytarska, K. Jaroch, K. Łuczykowski, J. Chałupka, J. Wietrzyk, K. Misiura, B. Bojko, S. Kruszewski and K. Z. Łączkowski, *Eur. J. Med. Chem.*, 2019, **175**, 162–171.
- 28 J. A. M. Damen, J. Escorihuela, H. Zuilhof, F. L. van Delft and B. Albada, *Chem.–Eur. J.*, 2023, **29**, e202300231.



- 29 A. Borrmann, O. Fatunsin, J. Dommerholt, A. M. Jonker, D. W. P. M. Löwik, J. C. M. van Hest and F. L. van Delft, *Bioconjug. Chem.*, 2015, **26**, 257–261.
- 30 J. A. M. Damen, J. Escorihuela, J. Firet, H. Zuilhof and B. Albada, *Chem. Sci.*, 2025, **16**, 23357–23365.
- 31 H. Chen, S. S. Ahsan, M. B. Santiago-Berrios, H. D. Abruña and W. W. Webb, *J. Am. Chem. Soc.*, 2010, **132**, 7244–7245.
- 32 Z. D. Baker, A. R. Thompson, D. D. Thomas and N. M. Levinson, *ACS Chem. Biol.*, 2025, **20**, 1683–1695.
- 33 A. M. Jones Brunette and D. L. Farrens, *Biochemistry*, 2014, **53**, 6290–6301.
- 34 T. G. Kapp, F. Rechenmacher, S. Neubauer, O. V. Maltsev, E. A. Cavalcanti-Adam, R. Zarka, U. Reuning, J. Notni, H.-J. Wester, C. Mas-Moruno, J. Spatz, B. Geiger and H. Kessler, *Sci. Rep.*, 2017, **7**, 39805.
- 35 D. Nakano, H. Watanabe, S. Kosuke and M. Ono, *Bioconjug. Chem.*, 2024, **35**, 1577–1586.

